Front. Earth Sci. 2020, 14(2): 479–491
https://doi.org/10.1007/s11707-019-0788-2

RESEARCH ARTICLE

# Changes in vegetation and moisture in the northern Tianshan of China over the past 450 years

**Weihe REN[1,2], Yan ZHAO[1,2], Quan LI (✉)[1], Jianhui CHEN[3]**

1 Key Laboratory of Land Surface Pattern and Simulation, Institute of Geographic Sciences and Natural Resources Research, Chinese Academy of Sciences, Beijing 100101, China
2 University of Chinese Academy of Sciences, Beijing 100049, China
3 Key Laboratory of West China's Environmental System (Ministry of Education), College of Earth and Environmental Sciences, Lanzhou University, Lanzhou 730000, China



**Abstract** Knowledge of historical changes in moisture within semi-arid and arid regions is the basis of climatic change predictions and strategies in response to long-term drought. In this study, a multiproxy peat record with high-resolution from Sichanghu in the northern Tianshan was used to document the changes in vegetation and climate over the past 450 years in the arid Central Asia. The pollen, grain size, and loss on ignition (LOI) records indicate that the productivity of local peat began to increase at ~1730 AD. The vegetation in the Sichanghu area experienced several transitions, from temperate desert to dense desert, marsh meadow, and steppe desert vegetation. The climate in the study area was extremely dry during the early stages of the Little Ice Age (LIA) (before 1730 AD) and relatively wet during the late stages (1730–1880 AD). The inferred changes in the moisture conditions of the Sichanghu peatland since the LIA may have been controlled by the extent of Arctic sea ice, the North Atlantic Oscillation, and the Siberian High via the connections of large-scale atmospheric circulations such as the Westerlies.

**Keywords** Little Ice Age, pollen, vegetation change, moisture condition, Tianshan, arid Central Asia

## 1 Introduction

Modern climate in the arid Central Asia (ACA) is sensitive to the intensity patterns of the Westerlies and the Asian Monsoon (AM) (Shi et al., 2006; Chen et al., 2015b; Huang et al., 2015a). The Westerlies plays an important role in the moisture supply for the ACA, given that summer precipitation can be traced to the western Eurasia including the closed Aral-Caspian Basin, the eastern Mediterranean, and the Black Sea (Aizen et al., 2006; Chen et al., 2010a; Huang et al., 2015a). The ACA's ecological system, agricultural yields, and local cultural shifts have been largely influenced by decennial-centennial hydrological fluctuations (Ferronskii et al., 2003; Buckley et al., 2010; Davi et al., 2015). Previous studies of this region have focused on reconstructing past changes in climate, applications and limitations of paleoclimate proxies, and the possible driving mechanism for decennial-centennial wet/dry oscillations at different time scales (Chen et al., 2008 and 2010a; Li et al., 2018).

Various proxies from peatland and lacustrine/eolian sediments have recently been used to reveal the histories of moisture and hydrological conditions in the ACA over the past few thousand years (Wu et al., 2004; Liu et al., 2011; Hong et al., 2015), including $\delta^{13}C$ record, lacustrine fossil diatom assemblages (Chiba et al., 2016), *n*-alkanes from peatland samples (Zhang et al., 2016), and fossil pollen assemblages from lake sediments or peatlands (Zhang et al., 2004 and 2015; Chen et al., 2006; Huang et al., 2015b). However, previous paleoclimate records have been inconsistent with respect to the moisture conditions in the Holocene epoch (Chen et al., 2008). For example, the variations in effective moisture in the Little Ice Age (LIA, ~1500–1850 AD, a notable cold interval), which have received widespread attention, are still debated.

In previous studies, wetter conditions have been reported for the ACA in the LIA (Chen et al., 2010a and 2015b), whereas relatively dry or inconspicuously humid conditions have been reconstructed for different intervals in the LIA (Hong et al., 2015; Zhang et al., 2016). For instance, the positive $\delta^{13}C$ obtained for peat cellulose in Chaiwobu indicated inadequate summer rainfall (Hong et al., 2015). Numerous studies have also indicated that the

Received May 4, 2019; accepted August 22, 2019

E-mail: liquan@igsnrr.ac.cn

LIA climate was unstable and represented by wet-dry transitions (Paulsen et al., 2003; Liu et al., 2011; Tian et al., 2013). Therefore, more high-resolution records of vegetation and climate changes are needed for a better understanding of the changes in moisture and hydrological conditions during key periods, and a better prediction of ecosystem and precipitation responses to anthropogenic climate change (Cao et al., 2015).

Peatlands in western China are valuable archives for the study of past hydrological changes (Hong et al., 2015; Zhang et al., 2015 and 2016). The initiation of basal peats in the ACA (e.g., Altai and Sichanghu) and on the Tibetan Plateau can be traced to the early Holocene (Zhang et al., 2009 and 2016; Hong et al., 2015; Zhao et al., 2014). Pollen records of peat profiles were widely applied to recover the high-resolution vegetation successions and climatic changes (Chen et al., 2006; Zhang et al., 2009 and 2015; Zhao et al., 2011; Huang et al., 2015b). However, there is a lack of high-resolution pollen records for ACA, which limits our knowledge of climatic changes in the region and the related responses of the ecological system during the LIA.

The northern Tianshan (a.k.a., the Tian Mountains) is located in the core area of the Westerlies-dominated climate regime (Chen et al., 2019). A previous study of an eolian sedimentary profile from the Sichanghu area in the northern Tianshan showed that the local vegetation underwent significant turnover from desert to marsh meadow and then to desert in the last millennium (Zhang et al., 2009). However, the low resolution of the pollen record and poor age control in this region have limited our knowledge about how the vegetation would respond to the past climate changes. Here, we present an integrated record of pollen, charcoal, sediment grain size, and the loss on ignition (LOI) from a peat profile (SCH) from the Sichanghu peatland. In our study, we aimed to recover the changes in vegetation and climate over the past 450 years in the northern Tianshan and to explore the mechanisms underlying climatic changes during the LIA in the ACA.

## 2 Materials and methods

### 2.1 Regional setting

The Sichanghu peatland is located in the northern Tianshan, where the regional precipitation is currently controlled by the Westerlies (Fig. 1). The peatland formed in an ancient marsh, which covered an area of ~20 km$^2$ before the lake dried up (Yan et al., 2003; Zhang et al., 2009). The mean annual temperature (MAT) is ~5.3°C, and the mean annual precipitation (MAP) is as low as ~129 mm. More than 43% of the rainfall occurs during summer (Fig. 2). Moisture is the dominant factor controlling the successions and distributions of different vegetation in the region. Temperate desert vegetation occupies the Sichanghu area and primarily contains members of the Chenopodiaceae (*Salsola*, *Suaeda physophora*, and *Haloxylon ammodendron*), Cyperaceae sedges, the Poaceae (*Festuca*), *Artemisia*, and the Ephedraceae (Luo et al., 2009; Yang et al., 2016). An altitudinal vegetation belt developed in the highlands and on the slopes of the surrounding mountains, including a temperate

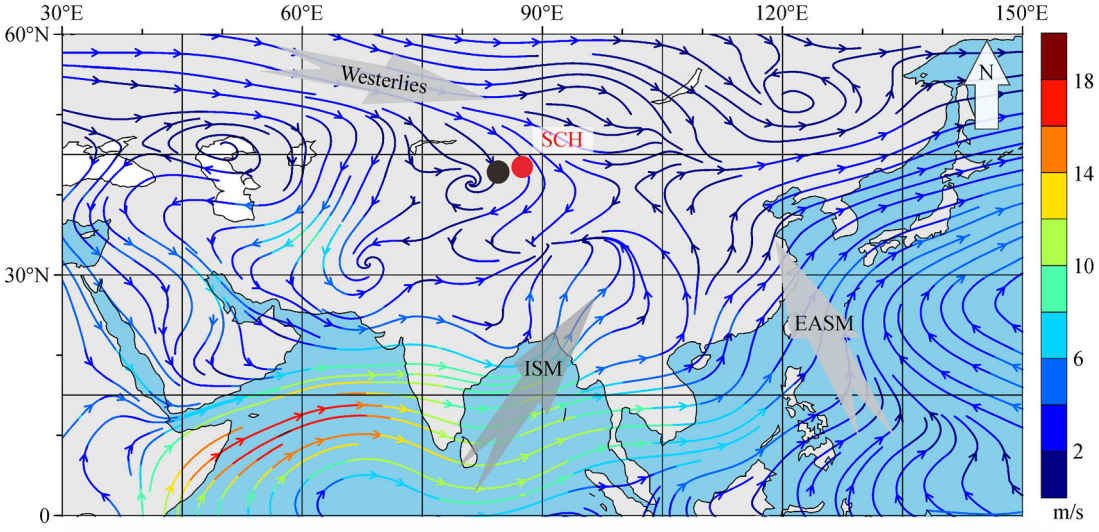


**Fig. 1** Location of the SCH profile in the arid Central Asia. The tree rings from the Central Tianshan (Chen et al., 2015a; black dot) and the June-July-August (JJA) streamline of the mean 850 hPa (reanalysis data during 1979–2010, data from the National Centers for Environmental Prediction/National Center for Atmospheric Research) were exhibited. EASM = East Asian Summer Monsoon; ISM = Indian Summer Monsoon.

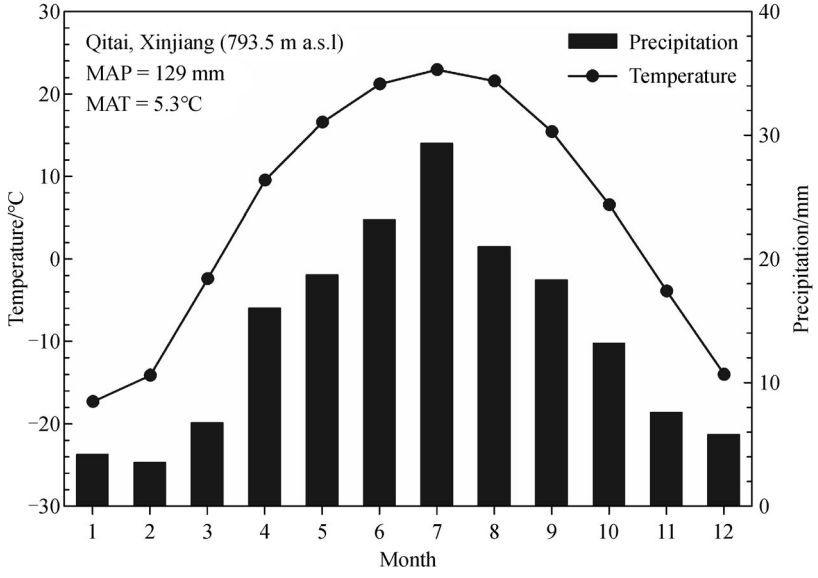


**Fig. 2** Modern climate conditions recorded by the Qitai Meteorological Station (from 1961 to 2015) in the vicinity of Sichanghu area.

desert (mainly consisting of *Artemisia*), spruce forest (primarily containing *Picea schrenkiana*), subalpine meadow (consisting of *Festuca* and other Poaceae) and alpine cushion meadows (mainly composed of *Thylacospermum caespitosum* and *Potentilla biflora*) (Yang et al., 2016).

### 2.2 Sediment samples

During our field survey in August of 2011, a 92-cm profile (labeled as SCH, 44°06′29.2″N, 89°12′07.5″E, 616±3 m a.s.l.), composed of well-preserved peat layers overlain by silty loam sediments, was retrieved from the Sichanghu peatland (Fig. 4(a)). The top 52-cm of the profile consisted of a peat deposit, with the remainder, at depths of 53 to 92 cm consisting of a marsh deposit with dark silt. The SCH profile was subsampled at an interval of 1 cm for the analyses of grain size, LOI, and pollen assemblages, while the charcoal analysis used a 2 cm interval.

### 2.3 Dating and laboratory analyses

Five samples of sedge-leaves and seeds from different layers of the SCH profile were sent to Beta Analytic Inc. (Miami, USA) for accelerator mass spectrometry (AMS) $^{14}C$ dating. The results were calibrated using Calib v. 7.0 and IntCal13 data sets (Reimer et al., 2013). The age-depth model was established using the Bacon model (mL = 1 for WinBacon2.2) (Blaauw and Christen, 2011; R Code Team, 2012).

A total of 88 samples (0.5–3.0 g each) were used for LOI analyses. The samples were first dehydrated in an oven at 105°C for 12 h. Subsequently, the organic matter and carbonate contents were calculated using sequential combustion at 500°C and 1000°C and a muffle furnace (Dean, 1974; Heiri et al., 2001).

Samples for grain size analysis (~0.2 g each) were pretreated with 10 mL of 10% HCl, and then with 10 ml of 30% $H_2O_2$ to remove soluble salts and organic matters. They were placed together with 10 mL of $Na(PO_3)_6$ (0.05 mol/L) for 10 min to facilitate dispersion in an ultrasonic vibrator. After rinsing and the removal of suspended matter, the grain sizes of the samples were measured using a Mastersizer2000 analyzer (Malvern Panalytical Ltd., UK).

Eighty-eight samples (0.5–1.6 g each) were used for pollen analyses following the standard procedures of Fægri and Iversen (1989). One tablet with a known-number of *Lycopodium* spores was added to each sample to estimate pollen concentration. Identification of the pollen taxon was performed by consulting the published literature (Wang, 1995). The mean number of counted pollen for each sample was 450 grains. The pollen percentage was estimated based on the total number of terrestrial pollen grains. The pollen zonation was determined with the help of stratigraphically constrained cluster analyses of the CONISS program (Grimm, 1987). Principal component analysis (PCA) was then applied to the pollen data ( $>2\%$ in at least one sample) to extract the main variations in the vegetation using CANOCO 4.5 (Ter Braak and Šmilauer, 2002). Pollen-based biomization was utilized to quantitatively reconstruct the vegetation occupying the landscape of our studied area (Prentice et al., 1996), which includes the assignment of modern pollen taxa to pollen functional types (PFTs), and the PFTs to different biomes according to the description on the modern pollen database of China (Chen et al., 2010b). The pollen-based biomization

analysis was conducted with software 3Pbase (Guiot and Goeury, 1996).

## 3 Results

### 3.1 Stratigraphy and chronology

The stratigraphy of the SCH profile is summarized in Fig. 4. The top 52 cm consisted of peat deposits, while the bottom was composed of dark gray silty clay (at depths from 52 to 92 cm). The development of the age-depth model was based on five AMS $^{14}$C dates (Table 1). The surface sample had a calibrated age of 2011 AD, corresponding to the time of sampling. The dating results showed that the SCH profile covers the past 450 years. The sedimentation process was relatively stable with a rate of ~0.20 mm/yr (Fig. 3).

### 3.2 Results of grain size and LOI analyses

Results of grain size analyses revealed that significant variations have occurred since 1560 AD (Figs. 4(b) and 4(c)). The mean grain size was much finer after 1740 AD, with the finest interval observed between 1740 and 1880 AD. Fluctuations in the mean grain size were correlated with the lithological transition from marsh sediments to peat deposits at ~1740 AD.

The results of the LOI analyses revealed that the SCH profile was dominated by organic matter (3%–72%) and silicates (32%–92%) (Figs. 4(d) and 4(f)), while the carbonate content was very low (1%–10%) throughout the entire profile (Fig. 4(e)). The well-preserved peat in the top 52 cm (1740–2011 AD) had a high organic matter content (~40%) but low silicate content ( < 50%), while the marsh sediments in the bottom (1520–1740 AD) of the profile exhibited a high abundance of silicates (~89%), but little

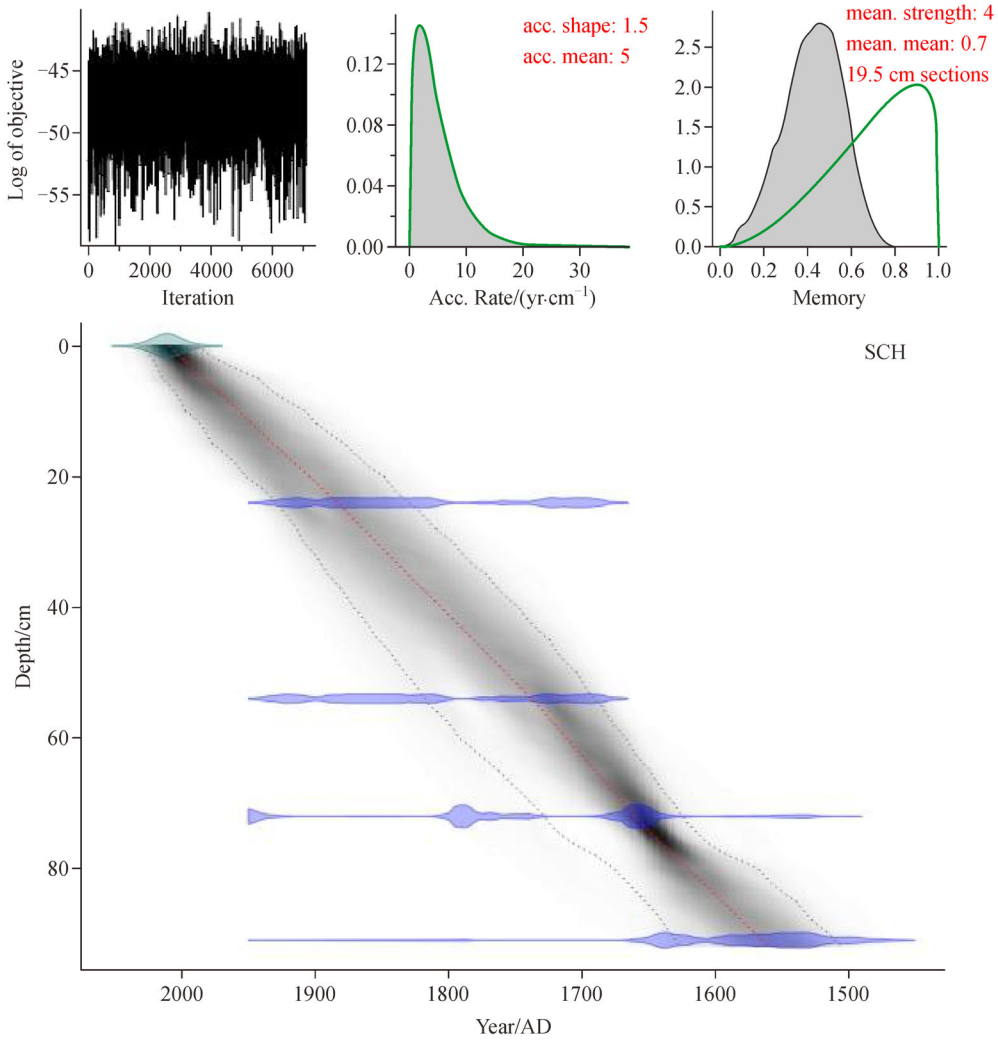


**Fig. 3** Chronology result for the SCH profile based on the Bacon model. The shaded region shows the error ranges (90%) of the model permutations. Acc. = acceleration.

**Table 1** Accelerator mass spectrometry (AMS) $^{14}C$ dates and calibration of the SCH profile

| Sample Code | Depth/cm | Material | $\delta^{13}C$/(‰ PDB) | $^{14}C$ age±standard deviation/yr BP | Calibrated age (2 Sigma, cal. year CE) | Probability |
|---|---|---|---|---|---|---|
| Beta-383641 | 24 | Sedge leaves | −26.5 | 110±30 | 1802–1938 | 0.694 |
| Beta-417756 | 54 | Sedge seeds | – | 120±30 | 1679–1939 | 1 |
| Beta-383643 | 72 | Sedge leaves | −26.9 | 230±30 | 1636–1805 | 0.909 |
| Beta-389554 | 72 | Sedge seeds | −24.5 | 220±30 | 1642–1805 | 0.889 |
| Beta-383644 | 91 | Sedge leaves | −27.3 | 300±30 | 1490–1602 | 0.729 |

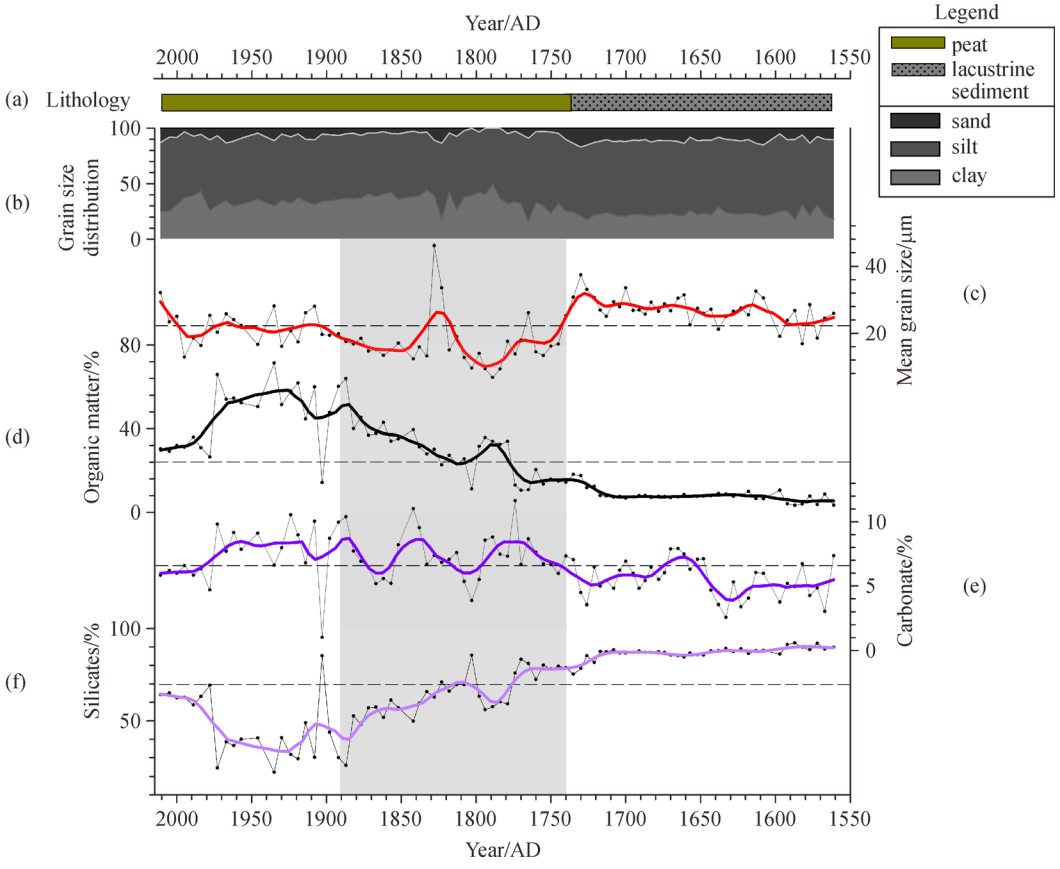


**Fig. 4** Lithology and records of grain size and LOI indices of the SCH profile. (a) Lithology; (b) Grain size distribution (as the grain size of sand > 64 μm), that of silt within 4–64 μm, and that of clay < 4 μm); (c) Mean grain size (μm); (d) Content of organic matter (%); (e) Content of carbonate (%); (f) Content of silicates (%).

organic matter (< 10%). The organic matter content reached a maximum at a depth of 8–22 cm (~1880–1970 AD).

### 3.3 Pollen record

In total, 49 pollen types were distinguished in the SCH profile at a temporal resolution of ~5 yr. The pollen assemblages were dominated by the Chenopodiaceae (~20%–80%), Cyperaceae (mean = 9%), *Artemisia* (8%), and Poaceae (6%). These assemblages could be divided into four pollen zones (Fig. 5). Two major biomes, including desert vegetation (H) and steppe vegetation (G) exhibited higher affinity scores than those of other biomes. Desert vegetation was the dominant type throughout the past 450 years, while steppe vegetation dominated the SCH-3 zone.

#### 3.3.1 Zone SCH-1 (depth of 92–84 cm, 1561–1600 AD)

Zone SCH-1 is characteristic with high percentages of Chenopodiaceae pollen (mean 75%) and low *Artemisia*/

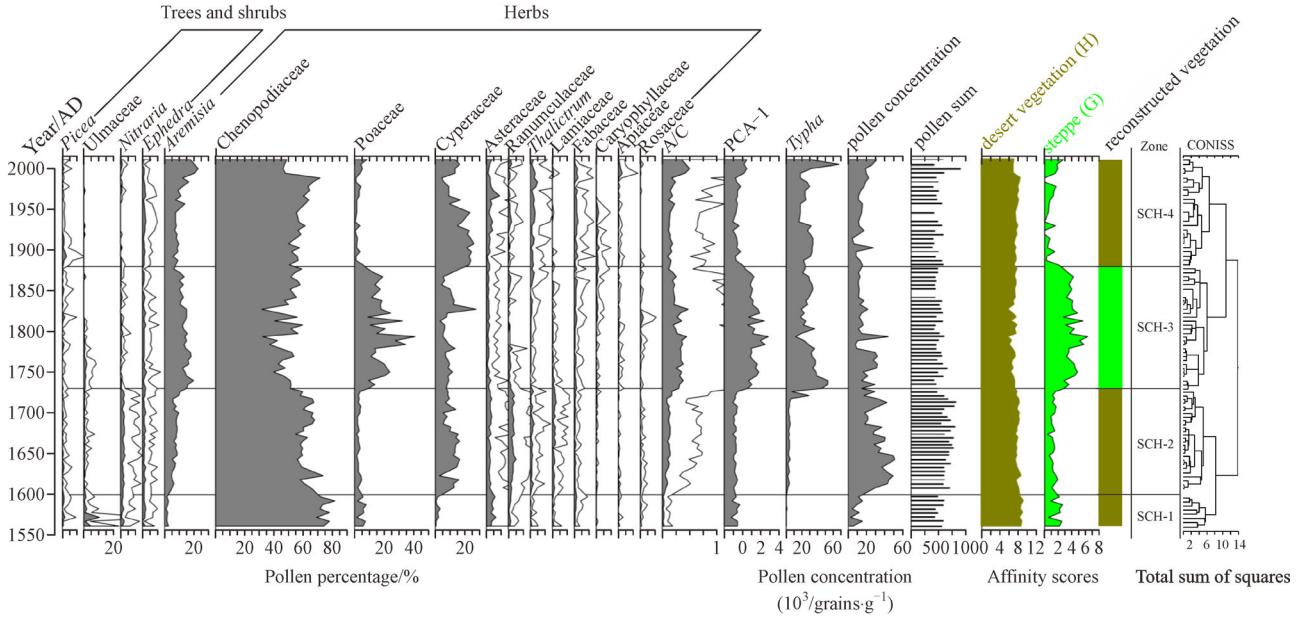


**Fig. 5** Pollen percentage diagram of the SCH profile. Only major taxa and the dominant biomes, such as desert vegetation and steppe, are shown. The open curves indicate 5 × exaggerations.

Chenopodiaceae (A/C) ratios (~0.03). *Typha* pollen are absent in this pollen zone. The pollen concentrations fluctuate between 2000 and 22000 grains/g.

### 3.3.2 Zone SCH-2 (84–56 cm, 1600–1730 AD)

The pollen assemblages of Zone SCH-2 are characterized by abundant Chenopodiaceae (~60%), Cyperaceae (up to 16%), and *Artemisia* (~7.3%). The A/C ratios are constant (~0.1). The pollen concentrations increase relative to Zone SCH-1 to 22000–65000 grains/g.

### 3.3.3 Zone SCH-3 (56–25 cm, 1730–1880 AD)

Zone SCH-3 features a sharp decrease in Chenopodiaceae pollen (34.6%), while *Typha* (up to 53%) and Poaceae taxa (reaching a maximum of 40%) show significant increases. The *Artemisia* content gradually increases (~9.9%), while that of Cyperaceae decreases to 7%. Consequently, the A/C ratios increase to ~0.25. The pollen concentrations fluctuate, but generally increase to 6000–70000 grains/g.

### 3.3.4 Zone SCH-4 (25–0 cm, 1880–2011 AD)

The pollen assemblages of Zone SCH-4 are dominated by high contents of Chenopodiaceae (57%), Cyperaceae (~15%), and *Artemisia* (~10%). The Poaceae concentration decreases to 3%. The A/C ratios are higher (~0.27) and reach a maximum of 0.56 in this zone. The pollen concentrations typically fluctuate around ~15000 grains/g.

## 3.4 Principal component analysis

The PCA results for pollen samples and major taxa could reveal their ordinations and characteristics along an ecological/environmental gradient (Fig. 6). The first two principal components (PC-1 and PC-2) capture 40.28% and 26.54% of the total variance in the pollen data,

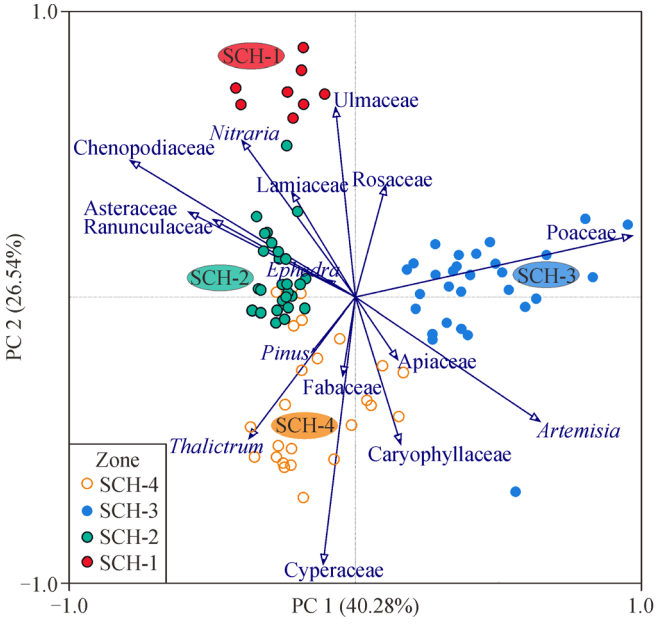


**Fig. 6** Results of principal component analysis of samples and major pollen taxa for SCH profile.

respectively. The drought-tolerant taxa, such as the typical desert taxa of Chenopodiaceae, *Ephedra* and *Nitraria*, are distributed in the negative direction of PC-1 (Fig. 6), while moisture-favoring steppe taxa, like *Artemisia* and Poaceae, in the positive direction. This suggests that PC-1 might represent the gradient in the moisture conditions. Furthermore, the PCA plots of the samples support the CONISS-based zonation of the pollen zones: SCH-1 (1561–1600 AD), SCH-2 (1600–1730 AD), SCH-3 (1730–1880 AD), and SCH-4 (1880–2011 AD) (Fig. 5).

## 4 Discussion

### 4.1 A/C ratio as an index of moisture

The pollen assemblages of the SCH profile are dominated by Chenopodiaceae (20%–80%) and *Artemisia* (2%–15%). In arid and semi-arid China, the pollen ratio of A/C is typically used as an indicator of steppe-desert vegetation transitions and effective moisture, either in investigations of the relationship between modern pollen assemblage and the contemporary vegetation (Herzschuh, 2007; Luo et al., 2009; Li, 2012; Zhao et al., 2012a and 2012b; Wei and Zhao, 2016; Ma et al., 2017) ,or in the paleo-environment reconstructions (Zhang et al., 2009; Zhao et al., 2010; An et al., 2012). Comparisons among the MAP data recorded by the nearby Qitai Meteorological Station, PC-1 scores, and A/C ratios of our study, exhibited similar variations over the past 50 years. A stable stage before the 1970s, a gradual increase before 2000, and a slight decrease within the last ten years were observed (Fig. 7). Therefore, A/C ratio can be used as a reliable indicator of effective moisture in the Sichanghu region (Herzschuh, 2007), wherein lower A/C ratios can reflect desert-like vegetation and less effective moisture/precipitation, and vice versa (Herzschuh, 2007; Yang et al., 2016).

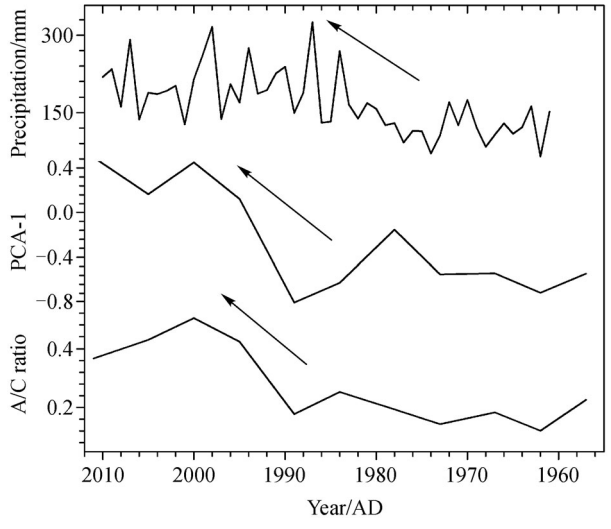


**Fig. 7** Comparisons among the A/C ratio, PCA-1 scores from the SCH profile, and the MAP data from the adjacent Qitai Meteorological Station (available at CMA website). Arrows indicate the overall trends toward the present.

### 4.2 Pollen-inferred vegetation and climate history

Based on the variations of pollen assemblages and A/C ratios, the environment in the northern Tianshan, over the past 450 years could be subdivided into four stages (Figs. 5 and 8).

From 1561 to 1600 AD (Stage 1), temperate desert vegetation and a drought conditions prevailed in the Sichanghu area, as indicated by the predominance of Chenopodiaceae pollen, low A/C ratios, low pollen concentrations, and very coarse sediments.

From 1600 to 1730 AD (Stage 2), steppe vegetation consisting of *Artemisia* and Cyperaceae increased in the representation of both the pollen assemblage and regional vegetation, although Chenopodiaceae was dominant. The desert vegetation in the vicinity of the Sichanghu peatland increased in density, as suggested by the increasing pollen concentration. During this stage, there was an increase in humidity.

From 1730 to 1880 AD (Stage 3), *Artemisia*, Poaceae, and Cyperaceae accounted for the majority of the pollen assemblages and vegetation composition, while the Chenopodiaceae content suddenly reduced to the lowest of the profile. Poaceae pollen of this stage was a typical taxon of wetland vegetation and temperate steppe in the Qaidam Basin and the northern Tianshan (Zhao et al., 2010), rather than an index of cultivated crops (Qin et al., 2011). The *Typha* pollen and A/C ratio showed sharp increases during this period. Steppe vegetation was indicated by the abundant Poaceae, *Artemisia*, and Cyperaceae pollen and the high affinity score of steppe in this stage (Fig. 5). It is suggested that regional vegetation of steppe and marsh meadow patches began to develop in the mid-1700s (Fig. 5), as indicated by high proportions of Poaceae, the lithological transition from lacustrine sediments to peat deposit, and an increase in organic matter content (Fig. 4), as well as the lowest range of grain size (Fig. 8). The initial SCH peatland (lowland at 616 m a.s.l.) was developed later than most other peatlands in the ACA (e.g., Chaiwobu peat at ~1000 m a.s.l., Hong et al., 2015; Tielishahan peat at 1770 m a.s.l., Zhang et al., 2016). This could be attributed to the precipitation effect along an altitudinal gradient (Zhao et al., 2010; Rao et al., 2019). The cold climatic interval in the 1800s was confirmed by previous studies (Mann et al., 2009), which could be coincident with the LIA in most regions of China (Wang et al., 1998; Yang et al., 2002). Overall, the Sichanghu area experienced a cold-wet climate in this period, during which a local marsh meadow occupied the landscape leading to high peat productivity.

From 1880 to 2011 AD (Stage 4), the vegetation type

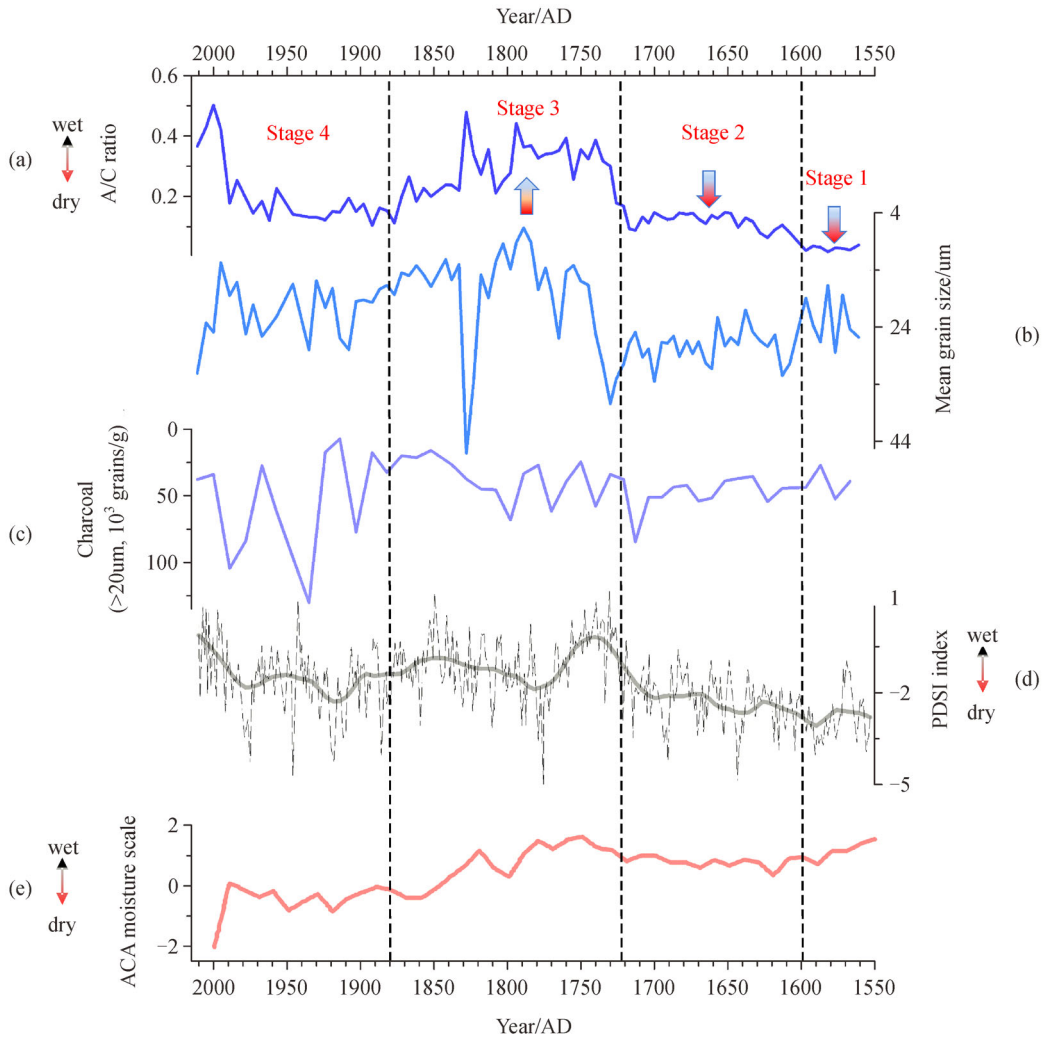


**Fig. 8** Correlations among the SCH records and other paleoclimate records in the vicinity. (a) A/C ratio; (b) Mean grain size; (c) Charcoal concentration in this study; (d) Palmer Drought Severity Index (PDSI) in central Tianshan (Chen et al., 2015a); (e) Synthesized effective moisture changes in ACA (Chen et al., 2010a).

changed to that of a steppe desert, as indicated by the dominance of Chenopodiaceae, Cyperaceae, and *Artemisia* pollen, in addition to the sudden decrease of Poaceae pollen. The high *Typha* content, A/C ratio, and organic matter content indicate that the climate remained humid during this period. The vegetation and climate began to degrade in the 2000s as reflected by our records and the observed meteorological data (Figs. 4–7).

The temperature in the early LIA was higher than during the late LIA, which could have induced more negative precipitation/evaporation (P/E) ratios (Chen et al., 2019), and thus relatively dry conditions for the terrestrial environment which was indicated by low A/C pollen ratios (Fig. 8). However, the water level may also have been higher during the early LIA, even though the lake was drying up. Therefore, the lacustrine sediments were deposited during the early LIA. After the extinction of the lacustrine environment, the more positive P/E ratios of the late LIA led to an increase in effective moisture (indicated by high A/C ratios) for the terrestrial vegetation (Fig. 8(a)). Low temperatures could also have enhanced the preservation of plant litter to form abundant peat deposits.

Overall, based on the pollen records and biome reconstructions, the vegetation in the Sichanghu area experienced several transition, first from a temperate desert to a dense desert, then to a marsh meadow, and finally to a steppe desert. The climate sharply transitioned from extremely dry to relatively wet conditions at ~1730 AD, resulting in an increase in peat productivity.

### 4.3 Inferred climatic changes and possible mechanisms

The moisture conditions during the LIA varied spatially

across the ACA (Chen et al., 2010a and 2015b). The wet climate of the LIA was reported in numerous previous studies, including the ice accumulation record of Guliya (Yao et al., 1996a), the lacustrine records of carbonate content in Lake Bosten (Chen et al., 2006), the sediment salinity record in Lake Sugan (Chen et al., 2009), the $\delta^{13}C$ record from the Tarim Basin (Liu et al., 2011), and the lacustrine biomarker record in Lake Manas (Song et al., 2015). Our multiproxy data of the SCH profile revealed two major stages of the LIA climate: 1) an extremely dry climate before ~1730 AD (early LIA), and 2) a relatively wet climate from 1730 to 1880 AD (late LIA).

#### 4.3.1 Extremely dry climate in the early LIA

The climate in the Sichanghu area was extremely dry before ~1730 AD, as inferred from the lowest A/C ratios (Fig. 8(a)). This is also supported by other records from the nearby regions. Data obtained from the Belukha ice core from Southern Siberia indicated exceptionally dry conditions during the 1600s and 1700s, as reflected by a high dust concentration, widespread forest diebacks, and frequent fire events (Eichler et al., 2011). During the early LIA, the dry conditions were considered to be closely related to the positive mode of the Pacific Decadal Oscillation (PDO) (Eichler et al., 2011). A dry stage during the 1600s was also indicated by low glacial accumulation (Yao et al., 1996a) and high $Mg^{2+}$ contents found in the Guliya ice core (Yang et al., 2006). Furthermore, the negative Palmer Drought Severity Index (PDSI) reflected by tree rings from the central Tianshan also revealed a drought interval during the early LIA, which was probably linked to El Niño-Southern Oscillation (ENSO) and North Atlantic Oscillation (NAO) (Fig. 8(d)) (Chen et al., 2015a). Other records, such as the low sea levels reconstructed in the Caspian Sea (Beni et al., 2013) and low lake level in the Lake Manas from ~1550–1700 AD (Song et al., 2015), were attributed to an increasing solar irradiance and the related humidity decrease during the LIA.

#### 4.3.2 Wet climate in the late LIA

The high A/C ratios, high organic matter content in the peat deposits (Figs. 4(d) and 8(a)), and abundant hydrophytic pollen from *Typha* observed from 1730 to 1880 AD (Figs. 4(c) and 5), as well as the occupation of a marsh meadow (Fig. 5), indicate a relatively wet climate for the late LIA. Furthermore, the moisture proxy of the A/C ratio was slightly opposite to the temperature on the centennial scale during the LIA (Fig. 9). However, dating uncertainties might exist in these hydroclimatic records in arid areas of China (Chen et al., 2015b).

According to most studies, a relatively wet climate in the late LIA was reported in the ACA (Fig. 8(e)). These studies included data from a set of tree rings indicating a humid late LIA in the central Tianshan (Fig. 8(d)); (Chen et al., 2015a), and an increasing ice accumulation rate after 1700 AD, recorded by Dunde and Guliya ice cores (Yao et al., 1996b; Wang et al., 2007). However, other hydro-climatic records had shown an inconspicuously humid climate in the late LIA (Zhang et al., 2009; Hong et al., 2015). Overall, the amplitude and timing of the moisture conditions during the LIA in the ACA remain debated.

#### 4.3.3 Climatic change after the LIA

The effective moisture recorded in the Sichanghu area from 1880 to 2011 AD (Stage 4) is generally consistent with previous climate records from other sites in the ACA. Compared to Stage 3, the lower A/C ratio and higher content of charcoal fragments in Stage 4 suggest a relatively dry climate. This period of climatic deterioration was also recorded by a tree ring record in the Tianshan (Fig. 8(d)) (Chen et al., 2015a). It has been suggested that dry climatic conditions prevailed in most areas of the ACA after the LIA (Fig. 8(e)) (Chen et al., 2010a).

#### 4.3.4 Possible forcing mechanism for climate change in Sichanghu

In this study, the moisture changes in the Sichanghu area over the past 450 years, NAO (Cook et al., 2002; Trouet et al., 2009), climate factors of the high northern latitudes (i.e., Siberian High SLP proxy and Barents-Kara Sea ice extent) (Meeker and Mayewski, 2002; Zhang et al., 2018), and reconstructed temperature variations (PAGES 2k Consortium, 2013) were correlated in order to explore the possible driving forces responsible for the LIA climate changes in the ACA (Fig. (9)). The changes in moisture condition in the Sichanghu peatland showed a negative correlation with that in the NAO (Cook et al., 2002; Trouet et al., 2009) (Fig. 9(d)), but a positive correlation with the Barents-Kara sea ice extent in autumn (Fig. 9(b)) (Zhang et al., 2018). However, dating uncertainty might exist among different records.

Previous studies suggest that negative phase of the NAO and increased Barents-Kara sea ice extent may have triggered an increase in precipitation during the LIA in Westerlies-dominated Asia (Hurrell, 1995; Chen et al., 2006, 2010a and 2015b). Increased snow cover in the Arctic Ocean is positively correlated with enhanced precipitation over Asia (Cohen et al., 2014), while the intensity of the winter Siberian High showed a significant negative correlation with the Barents-Kara sea ice anomalies from autumn to winter (Wu et al., 2011) (Figs. 9(c) and 9(b)). In fact, some observations have confirmed a negative correlation between the Barents-Kara sea ice extent and the phase of the NAO (Cohen et al., 2014). Complex driving forces were responsible for the

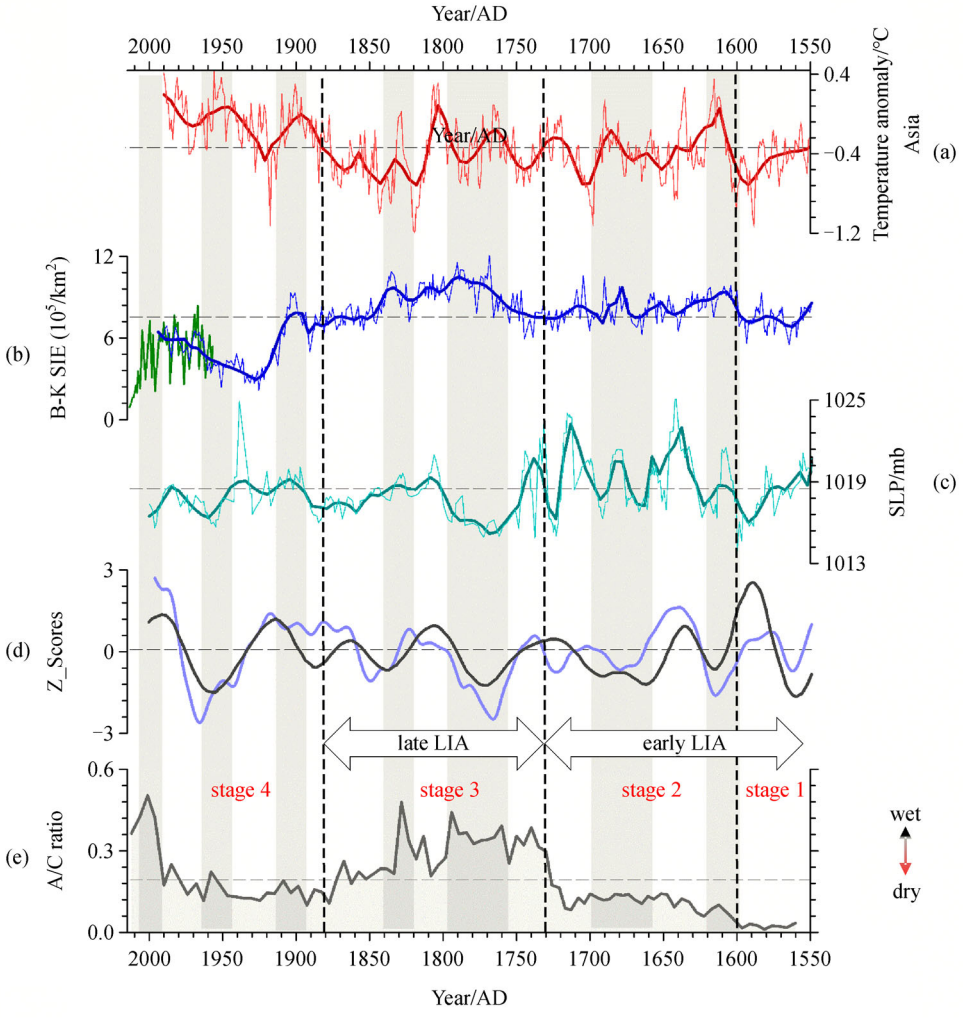


**Fig. 9** Correlations among the SCH records and other worldwide paleoclimate records. (a) Temperature reconstruction for Asia (PAGES 2k Consortium, 2013); (b) observed (dark green curve) and reconstructed changes in sea ice extent during autumn in the Barents-Kara Sea (blue curve) (Zhang et al., 2018); (c) Siberian High sea level pressure (SLP) proxy (Meeker and Mayewski, 2002); (d) reconstructed North Atlantic Oscillation (NAO, light blue curve following Trouet et al., 2009; black curve following Cook et al., 2002); (e) A/C ratio variations in the SCH profile (this study). The gray shaded bars indicate the relatively wet intervals since the 1550s.

changes in moisture conditions during the late LIA. For example, the relatively wet conditions were attributable to the low solar irradiance at the Maunder (1650–1710 AD) and Dalton minima (1790–1830 AD) (Lean, 2000). The low temperatures during the LIA could result in less evaporation and thus more effective moisture in the region (Chen et al., 2010a).

In summary, the Arctic sea ice extent, NAO phase, and Siberian High, closely correlated through the connection of atmospheric circulation (Raible et al., 2007; Chen et al., 2010a, 2015a, 2015b, and 2019), could be responsible for the changes in moisture conditions in the ACA during the LIA. The low Siberian High and the peak ice extent of Barents-Kara sea in the late LIA could have caused the wet climate during the late LIA in the northern Tianshan (Fig. 9, Stage 3). However, more detailed investigations and high-resolution climate records are still needed for a better understanding of the interactions among the different climate drivers responsible for the moisture variations in the ACA.

## 5 Conclusions

In this study, a multiproxy record of vegetation and climate changes in Sichanghu peatland over the past 450 years was developed. The pollen assemblages, grain sizes, and LOI records indicated that the peat deposit was initially formed at ~1730 AD. Based on biomization results, the vegetation in the Sichanghu area underwent transitions from temperate desert (1561–1600 AD) to dense desert (1600–1730 AD), steppe (1730–1880 AD), and steppe desert vegeta-

tion (1880–2011 AD).

According to the variations of the A/C pollen ratio, the climate in the Sichanghu area was extremely dry before 1730 (early LIA), and relatively wet from 1730 to 1880 AD (late LIA). The inferred changes in moisture conditions may have been controlled by the ice extent of the Arctic sea, NAO phase, and Siberian High through the connections of large-scale atmospheric circulation, such as the Westerlies. The mechanisms underlying the long-distance transport of moisture in the ACA and the key role of the atmospheric circulation between northern and high latitudes and the ACA should be further investigated.

**Acknowledgements** This work was supported by the National Natural Science Foundation of China (Grant Nos. 41690113, 41977395, 41671202 and 41471169), the Strategic Priority Research Program of the Chinese Academy of Sciences (No. XDA20070101), and the National Key Research and Development Program of China (Grant No. 2016YFA0600501). We wish to thank the anonymous reviewers, and Qiaoyu Cui, Feng Qin and Jie Xu for valuable suggestions.

## References

Aizen V B, Aizen E M, Joswiak D R, Fujita K, Takeuchi N, Nikitin S A (2006). Climatic and atmospheric circulation pattern variability from ice-core isotope/geochemistry records (Altai, Tien Shan and Tibet). Ann Glaciol, 43(1): 49–60

An C B, Lu Y B, Zhao J J, Tao S C, Dong W M, Li H, Jin M, Wang Z L (2012). A high-resolution record of Holocene environmental and climatic changes from Lake Balikun (Xinjiang, China): implications for Central Asia. Holocene, 22(1): 43–52

Beni A N, Lahijani H, Harami R M, Arpe K, Leroy S A G, Marriner N, Berberian M, Andrieu-Ponel V, Djamali M, Mahboubi A, Reimer P J (2013). Caspian Sea level changes during the last millennium: historical and geological evidence from the south Caspian Sea. Clim Past, 9(4): 1645–1665

Blaauw M, Christen J A (2011). Flexible paleoclimate age-depth models using an autoregressive gamma process. Bayesian Anal, 6(3): 457–474

Buckley B M, Anchukaitis K J, Penny D, Fletcher R, Cook E R, Sano M, Nam C, Wichienkeeo A, Minh T T, Hong T M (2010). Climate as a contributing factor in the demise of Angkor, Cambodia. Proc Natl Acad Sci USA, 107(15): 6748–6752

Cao X Y, Herzschuh U, Ni J, Zhao Y, Bohmer T (2015). Spatial and temporal distributions of major tree taxa in eastern continental Asia during the last 22,000 years. Holocene, 25(1): 79–91

Chen F H, Chen J H, Holmes J, Boomer I, Austin P, Gates J B, Wang N L, Brooks S J, Zhang J W (2010a). Moisture changes over the last millennium in arid Central Asia: a review, synthesis and comparison with monsoon region. Quat Sci Rev, 29(7–8): 1055–1068

Chen F H, Huang X Z, Zhang J W, Holmes J A, Chen J H (2006). Humid Little Ice Age in Central Asia documented by Bosten Lake, Xinjiang, China. Sci China Earth Sci, 49(12): 1280–1290

Chen F, Yuan Y J, Wei W S, Yu S L, Zhang T W, Shang H M, Zhang R B, Qin L, Fan Z A (2015a). Tree-ring recorded hydroclimatic change in Tianshan mountains during the past 500 years. Quat Int, 358: 35–41

Chen F, Yu Z, Yang M, Ito E, Wang S, Madsen D B, Huang X, Zhao Y, Sato T, John B. Birks H, Boomer I, Chen J, An C, Wünnemann B (2008). Holocene moisture evolution in arid Central Asia and its out-of-phase relationship with Asian monsoon history. Quat Sci Rev, 27 (3): 351–364

Chen F H, Chen J H, Huang W, Chen S Q, Huang X Z, Jin L Y, Jia J, Zhang X J, An C B, Zhang J W, Zhao Y, Yu Z C, Zhang R H, Liu J B, Zhou A F, Feng S (2019). Westerlies Asia and monsoonal Asia: spatiotemporal differences in climate change and possible mechanisms on decadal to sub-orbital timescales. Earth Sci Rev, 192: 337–354

Chen J H, Chen F H, Feng S, Huang W, Liu J B, Zhou A F (2015b). Hydroclimatic changes in China and surroundings during the Medieval Climate Anomaly and Little Ice Age: spatial patterns and possible mechanisms. Quat Sci Rev, 107: 98–111

Chen J H, Chen F H, Zhang E L, Brooks S J, Zhou A F, Zhang J W (2009). A 1000-year chironomid-based salinity reconstruction from varved sediments of Sugan Lake, Qaidam Basin, arid Northwest China, and its palaeoclimatic significance. Chin Sci Bull, 54(20): 3749–3759

Chen Y, Ni J, Herzschuh U (2010b). Quantifying modern biomes based on surface pollen data in China. Global Planet Change, 74(3–4): 114–131

Chiba T, Endo K, Sugai T, Haraguchi T, Kondo R, Kubota J (2016). Reconstruction of Lake Balkhash levels and precipitation/evaporation changes during the last 2000 years from fossil diatom assemblages. Quat Int, 397: 330–341

Cohen J, Screen J A, Furtado J C, Barlow M, Whittleston D, Coumou D, Francis J, Dethloff K, Entekhabi D, Overland J, Jones J (2014). Recent Arctic amplification and extreme mid-latitude weather. Nat Geosci, 7(9): 627–637

Cook E R, D'Arrigo R D, Mann M E (2002). A well-verified, multiproxy reconstruction of the winter North Atlantic Oscillation Index since A. D. 1400. J Clim, 15(13): 1754–1764

Davi N K, D'Arrigo R, Jacoby G C, Cook E R, Anchukaitis K J, Nachin B, Rao M P, Leland C (2015). A long-term context (931–2005 CE) for rapid warming over Central Asia. Quat Sci Rev, 121: 89–97

Dean W E (1974). Determination of carbonate and organic-matter in calcareous sediments and sedimentary-rocks by loss on ignition: comparison with other methods. J Sediment Petrol, 44(1): 242–248

Eichler A, Tinner W, Brütsch S, Olivier S, Papina T, Schwikowski M (2011). An ice-core based history of Siberian forest fires since AD 1250. Quat Sci Rev, 30(9–10): 1027–1034

Fægri K, Iversen J (1989). Textbook of Pollen Analysis. London: John Wiley and Sons

Ferronskii V I, Polyakov V A, Brezgunov V S, Vlasova L S, Karpychev Y A, Bobkov A F, Romaniovskii V V, Johnson T, Ricketts D, Rasmussen K (2003). Variations in the hydrological regime of Kara-Bogaz-Gol Gulf, Lake Issyk-Kul, and the Aral Sea assessed based on data of bottom sediment studies. Water Resour, 30(3): 252–259

Grimm E C (1987). CONISS: A Fortran 77 program for stratigraphically constrained cluster analysis by the method of incremental sum of squares. Comput Geosci, 13(1): 13–35

Guiot J, Goeury C (1996). PPPbase, a software for statistical analysis of

paleoecological and paleoclimatological data. Dendrochronologia, 14: 295–300

Heiri O, Lotter A F, Lemcke G (2001). Loss on ignition as a method for estimating organic and carbonate content in sediments: reproducibility and comparability of results. J Paleolimnol, 25(1): 101–110

Herzschuh U (2007). Reliability of pollen ratios for environmental reconstructions on the Tibetan Plateau. J Biogeogr, 34(7): 1265–1273

Hong B, Gasse F, Uchida M, Hong Y, Leng X, Shibata Y, An N, Zhu Y, Wang Y (2015). Increasing summer rainfall in arid eastern-Central Asia over the past 8500 years. Sci Rep, 4(1): 5279

Huang W, Feng S, Chen J H, Chen F H (2015a). Physical mechanisms of summer precipitation variations in the Tarim Basin in northwestern China. J Clim, 28(9): 3579–3591

Huang X Z, Chen C Z, Jia W N, An C B, Zhou A F, Zhang J W, Jin M, Xia D S, Chen F H, Grimm E C (2015b). Vegetation and climate history reconstructed from an alpine lake in central Tianshan Mountains since 8.5 ka BP. Palaeogeogr Palaeoclimatol Palaeoecol, 432: 36–48

Hurrell J W (1995). Decadal trends in the North Atlantic oscillation: regional temperatures and precipitation. Science, 269(5224): 676–679

Lean J (2000). Evolution of the Sun's spectral irradiance since the Maunder Minimum. Geophys Res Lett, 27(16): 2425–2428

Li G Q, Chen F H, Xia D S, Yang H, Zhang X J, Madsen D, Oldknow C, Wei H T, Rao Z G, Qiang M R (2018). A Tianshan Mountains loess-paleosol sequence indicates anti-phase climatic variations in arid Central Asia and in East Asia. Earth Planet Sci Lett, 494: 153–163

Li Y C (2012). Pollen-vegetation-climate relationship in some desert and steppe communities in Northern China. In: Schluchter C, Nietlispach J, XVIII INQUA Congress Abstracts, Quat Int, 279–280

Liu W G, Liu Z H, An Z S, Wang X L, Chang H (2011). Wet climate during the 'Little Ice Age' in the arid Tarim Basin, northwestern China. Holocene, 21(3): 409–416

Luo C X, Zheng Z, Tarasov P, Pan A D, Huang K Y, Beaudouin C, An F Z (2009). Characteristics of the modern pollen distribution and their relationship to vegetation in the Xinjiang region, northwestern China. Rev Palaeobot Palynol, 153(3–4): 282–295

Ma Q F, Zhu L P, Wang J B, Ju J T, Lü X M, Wang Y, Guo Y, Yang R M, Kasper T, Haberzettl T, Tang L Y (2017). *Artemisia*/Chenopodiaceae ratio from surface lake sediments on the central and western Tibetan Plateau and its application. Palaeogeogr Palaeoclimatol Palaeoecol, 479: 138–145

Mann M E, Zhang Z, Rutherford S, Bradley R S, Hughes M K, Shindell D, Ammann C, Faluvegi G, Ni F (2009). Global signatures and dynamical origins of the Little Ice Age and Medieval Climate Anomaly. Science, 326(5957): 1256–1260

Meeker L D, Mayewski P A (2002). A 1400-year high-resolution record of atmospheric circulation over the North Atlantic and Asia. Holocene, 12(3): 257–266

PAGES 2k Consortium (2013). Continental-scale temperature variability during the past two millennia. Nat Geosci, 6: 339–346 doi:10.1038/ngeo1797

Paulsen D E, Li H C, Ku T L (2003). Climate variability in central China over the last 1270 years revealed by high-resolution stalagmite records. Quat Sci Rev, 22(5–7): 691–701

Prentice I C, Guiot J, Huntley B, Jolly D, Cheddadi R (1996). Reconstructing biomes from palaeoecological data: a general method and its application to European pollen data at 0 and 6 ka. Clim Dyn, 12(3): 185–194

Qin J G, Taylor D, Atahan P, Zhang X R, Wu G X, Dodson J, Zheng H B, Itzstein-Davey F (2011). Neolithic agriculture, freshwater resources and rapid environmental changes on the lower Yangtze, China. Quat Res, 75(1): 55–65

Rao Z G, Wu D D, Shi F X, Guo H C, Cao J T, Chen F H (2019). Reconciling the 'westerlies' and 'monsoon' models: a new hypothesis for the Holocene moisture evolution of the Xinjiang region, NW China. Earth Sci Rev, 191: 263–272

Raible C C, Yoshimori M, Stocker T F, Casty C (2007). Extreme midlatitude cyclones and their implications for precipitation and wind speed extremes in simulations of the Maunder Minimum versus present day conditions. Clim Dyn, 28(4): 409–423

R Code Team (2012). R: A Language and Environment for Statistical Computing. Vienna: R Foundation for Statistical Computing

Reimer P J, Bard E, Bayliss A, Beck J W, Blackwell P G, Ramsey C B, Buck C E, Cheng H, Edwards R L, Friedrich M, Grootes P M, Guilderson T P, Haflidason H, Hajdas I, Hatté C, Heaton T J, Hoffmann D L, Hogg A G, Hughen K A, Kaiser K F, Kromer B, Manning S W, Niu M, Reimer R W, Richards D A, Scott E M, Southon J R, Staff R A, Turney C S M, van der Plicht J (2013). Intcal13 and marine13 radiocarbon age calibration curves 0–50000 years Cal BP. Radiocarbon, 55(4): 1869–1887

Shi Y F, Shen Y P, Kang E, Li D L, Ding Y J, Zhang G W, Hu R J (2006). Recent and future climate change in Northwest China. Clim Change, 80(3–4): 379–393

Song M, Zhou A F, Zhang X N, Zhao C, He Y X, Yang W Q, Liu W G, Li S H, Liu Z H (2015). Solar imprints on Asian inland moisture fluctuations over the last millennium. Holocene, 25(12): 1935–1943

Ter Braak C J F, Šmilauer P (2002). CANOCO Reference Manual and CanoDraw for Windows User's Guide: Software for Canonical Community Ordination (Version 4.5). Ithaca, NY: Microcomputer Power

Tian F, Herzschuh U, Dallmeyer A, Xu Q H, Mischke S, Biskaborn B K (2013). Environmental variability in the monsoon-westerlies transition zone during the last 1200 years: lake sediment analyses from central Mongolia and supra-regional synthesis. Quat Sci Rev, 73: 31–47

Trouet V, Esper J, Graham N E, Baker A, Scourse J D, Frank D C (2009). Persistent positive North Atlantic oscillation mode dominated the Medieval Climate Anomaly. Science, 324(5923): 78–80

Wang F X (1995). Pollen Morphology in China. Beijing: Science Press (in Chinese)

Wang N L, Jiang X, Thompson L G, Davis M E (2007). Accumulation rates over the past 500 years recorded in ice cores from the northern and southern Tibetan Plateau, China. Arct Antarct Alp Res, 39(4): 671–677

Wang S W, Ye J L, Gong D Y (1998). Climate in China during the Little Ice Age. Quat Sci, 18(1): 54–64 (in Chinese)

Wei H C, Zhao Y (2016). Surface pollen and its relationships with modern vegetation and climate in the Tianshan Mountains, northwestern China. Veg Hist Archaeobot, 25(1): 19–27

Wu B Y, Su J Z, Zhang R H (2011). Effects of autumn-winter Arctic sea ice on winter Siberian High. Chin Sci Bull, 56(30): 3220–3228

Wu J L, Liu J J, Wang S M (2004). Climatic change record from stable isotopes in Lake Aibi, Xinjiang during the past 1500 years. Quat Sci, 24(5): 585–590 (in Chinese)

Yan S, Kong Z C, Yang Z J (2003). Pollen analysis and its significance of the Sichanghu section in Jimusaer county, Xijiang. Acta Bot Bor-Occid Sin, 23(4): 531–536 (in Chinese)

Yang B, Braeuning A, Johnson K R, Shi Y F (2002). General characteristics of temperature variation in China during the last two millennia. Geophys Res Lett, 29(9): 1–4

Yang M X, Yao T D, Wang H J (2006). Microparticle content records of the Dunde ice core and dust storms in northwestern China. J Asian Earth Sci, 27(2): 223–229

Yang Z J, Zhang Y, Ren H B, Yan S, Kong Z C, Ma K P, Ni J (2016). Altitudinal changes of surface pollen and vegetation on the north slope of the Middle Tianshan Mountains, China. J Arid Land, 8(5): 799–810

Yao T D, Jiao K Q, Tian L D, Yang Z H, Shi W L, Thompson L G (1996a). Climatic variations since the Little Ice Age recorded in the Guliya ice core. Sci China Ser D Earth Sci, 39(6): 587–596

Yao T D, Thompson L G, Qin D H, Tian L D, Jiao K Q, Yang Z H, Xie C (1996b). Variations in temperature and precipitation in the past 2000 a on the Xizang (Tibet) Plateau-Guliya ice core record. Sci China Ser D Earth Sci, 39(4): 425–433

Zhang H, Zhang Y, Kong Z C, Yang Z J, Li Y M, Tarasov P E (2015). Late Holocene climate change and anthropogenic activities in north Xinjiang: evidence from a peatland archive, the Caotanhu Wetland. Holocene, 25(2): 323–332

Zhang Q, Xiao C D, Ding M H, Dou T F (2018). Reconstruction of autumn sea ice extent changes since 1289AD in the Barents-Kara Sea, Arctic. Sci China Earth Sci, 61(9): 1279–1291

Zhang Y, Kong Z C, Yan S, Yang Z J, Ni J (2004). “Medieval Warm Period” in Xinjiang—rediscussion on paleoenvironment of the Sichanghu profile in Gurbantunggut Desert. Quat Sci, 24(6): 701–708 (in Chinese)

Zhang Y, Kong Z C, Yan S, Yang Z J, Ni J (2009). “Medieval Warm Period” on the northern slope of central Tianshan Mountains, Xinjiang, NW China. Geophys Res Lett, 36(11): L11702

Zhang Y, Meyers P A, Liu X T, Wang G P, Ma X H, Li X Y, Yuan Y X, Wen B (2016). Holocene climate changes in the Central Asia mountain region inferred from a peat sequence from the Altai Mountains, Xinjiang, northwestern China. Quat Sci Rev, 152: 19–30

Zhao Y, Li F R, Hou Y T, Sun J H, Zhao W W, Tang Y, Li H (2012a). Surface pollen and its relationships with modern vegetation and climate on the Loess Plateau and surrounding deserts in China. Rev Palaeobot Palynol, 181: 47–53

Zhao Y, Liu H Y, Li F R, Huang X Z, Sun J H, Zhao W W, Herzschuh U, Tang Y (2012b). Application and limitations of the *Artemisia*/Chenopodiaceae pollen ratio in arid and semi-arid China. Holocene, 22(12): 1385–1392

Zhao Y, Yu Z C, Liu X J, Zhao C, Chen F H, Zhang K (2010). Late Holocene vegetation and climate oscillations in the Qaidam Basin of the northeastern Tibetan Plateau. Quat Res, 73(1): 59–69

Zhao Y, Yu Z C, Tang Y, Li H, Yang B, Li F R, Zhao W W, Sun J H, Chen J H, Li Q, Zhou A F (2014). Peatland initiation and carbon accumulation in China over the last 50,000 years. Earth Sci Rev, 128: 139–146

Zhao Y, Yu Z, Zhao W W (2011). Holocene vegetation and climate histories in the eastern Tibetan Plateau: controls by insolation-driven temperature or monsoon-derived precipitation changes? Quat Sci Rev, 30(9–10): 1173–1184